Chapter 5

Introduction

The ability of corroles to stabilize metals in high oxidation states led us to examine complexes with chromium as reported in the previous chapter. This resulted in rather stable, non reactive complexes. Previous experience in this group and others with iron and vanadium based catalysts has shown that reactivity can in general be increased by reducing the electron density of the ligand. [1-4]This was shown to be true for porphyrin as well as for salen-based compounds. In general, the increase in reactivity is counteracted by ligand deformation due to steric repulsion between electron withdrawing halogen groups. [5]This leads to a maximum in catalytic activity at less than full halogenation. [6-9]Due to the low reactivity of chromium corroles, it seemed worthwhile to determine if such a maximum also existed in order to ascertain the optimum degree of halogenation

Electrochemical behavior of the ligand can be used as a measure of both effects: the electron withdrawing effect is in general linearly dependent on the number of substituents, while disruption in the conjugation pathway of the macrocycle manifests itself by non-linear behavior. Partial bromination was first reported in the 1970s on free base porphyrin. [10]Due to the sensitivity of the free ligand, a better approach is to use a metallated ligand as starting material. Due to charge requirements for a neutral complex as well as electrochemical inertness, trivalent metals from the boron group are ideal. Theoretical work has shown that Ga(III) would be the ideal candidate[11] and such a corrole has indeed been reported.[12]

We thus decided to prepare and characterize a series of brominated corroles and study their electrochemical properties to ascertain the ideal degree of bromination.

Experimental

Materials

All chemicals were obtained either from Aldrich or EM Science (solvents) and used as received. $GaCl_3$ was kept under argon after opening. Tetrabutylammonium hexafluorophosphate was recrystallized from ethanol/ether. The ligand (tpfc)H_3 (**1**) was prepared according to literature procedures.

Electrochemistry

Voltammetric measurements were made on a CHI660 workstation with a normal three-electrode configuration, consisting of a glassy carbon electrode, an Ag/AgCl reference electrode, and a Pt-wire auxiliary electrode. Samples were in the mM range in 0.1 M $[Bu_4N]PF_6/CH_2Cl_2$ solution at room temperature.

Spectroscopy

UV-Vis spectra were taken on a HP 8452 spectrophotometer. NMR were obtained on either a 300 MHz (1D) or 500 MHz (2D) spectrometer.

Synthesis of (tpfc)Ga(py)

This compound was synthesized following the published procedure [12] by refluxing gallium chloride with the corrole ligand in boiling pyridine, followed by chromatographic purification.

Synthesis of (Br-tpfc)Ga(py)

20 mg of (tpfc)Ga(py) were dissolved with 4.4 mg NBS in 50 mL methanol and refluxed for 4 hrs. After removal of solvent, the residue was adsorbed on 2.5 g silica gel and loaded on a column (silica gel, 3 x 20 cm) and the first band eluted with hexanes/EtOAc was collected. (Gradient 240:10-200:50.) After removal of solvents, the residue was again adsorbed on silica gel and run down a column identical top the first one, but this time using hexanes/EtOAc/py 240:10:1 as eluant. The fractions were separated according to position of the Soret maximum into two. The later part contained the desired product which was obtained in 24 % yield (5.2 mg) after solvent removal. ^{1}H NMR (300 MHz) (CD_2Cl_2 δ in ppm): 9.30 (s, 1H), 9.24 (d, 1H, J=3.9 Hz), 8.90 (d, 1H, J=5.4 Hz), 8.89 (d, 1H, J=5.4 Hz), 8.84 (s, 1H, J=3.9 Hz)8.69 (2 d, 2H)

Synthesis of (Br_2-tpfc)Ga(py) and (Br_3-tpfc)Ga(py)

57 mg of (tpfc)Ga(py) were dissolved with 21.8 mg NBS in 50 mL methanol and refluxed for 4 hrs. After solvent removal, the residue was absorbed on 2.5 g silica gel and run down a column (silica gel IVa, 3x20 cm) using a gradient hexanes-hexanes/CH2CL2 220:30, and the first band was collected. The product was obtained after solvent removal in 20 % yield (13.2 mg) ^{1}H NMR (300 MHz) (CD_2Cl_2, δ in ppm): 9.28(d, 2H), 8.91(d, 2H), 8.70 (d, 2H).

The second band was eluted using hexanes/CH_2Cl_2 100:150. After solvent removal, it was readsorbed on silica gel and run through a second column, identical to the first one. The first band (eluted with hexanes/$CH_2Cl_2$200:50) was found to contain a mixture of partially brominated compounds. The second band (eluted with CH_2Cl_2) yielded (Br_3-

tpfc)Ga(py) in 11 % yield (8.2 mg) ^{1}H NMR. (300 MHz) (CD_2Cl_2, δ in ppm): 9.52(s, 1H), 8.88(d, 2H), 8.68 (d, 2H).

Synthesis of (Br$_7$-tpfc)Ga(py)

19.6 mg of (tpfc)Ga(py) were dissolved with 22.54 mg NBS in methanol and refluxed 4 hours. The residue obtained after solvent removal was adsorbed on 2 g of silica gel and run down a column (silica gel 3x20 cm) with hexanes/EtOAc/py 240:10:1. the bands were separated according to Soret absorption and the band absorbing at 434 (last band) was kept. After solvent removal, the residue was again run trough a column (silica gel IIIa, 3x20 cm). To band were eluted first using a hexanes/CH_2Cl_2 gradient (230-20-40:210).The desired product was then eluted using CH_2Cl_2 210:40 and obtained in 14 % yield (5 mg).

Results

Synthesis of partially brominated gallium corroles

The synthesis procedure was in itself pretty straightforward. The reactions are generally accompanied by a change in color from the purple of the starting material to bluish or green depending on the degree of bromination. The choice of bromination conditions (2, 4, and 6 equivalents, respectively) was dictated by the fact that we expected under- and over-bromination to occur, so that, for example, with two equivalents added, we would expect mono-, di-, and tri-bromo compounds to be formed. Analysis of the crude products by MS revealed this to be the case.

Therefore, the challenge was to devise a way to purify and identify the products. To distinguish between different degrees of bromination, we used ESI-MS. We found that this is a very useful tool to assess the purity of fractions(Figure 5.1). Unfortunately, this method cannot be used to tell isomers apart, let alone confirm their structures. Due to the small amounts of material prepared (generally <20 mg), we decided against using x-ray crystallography, and rather use NMR to check for isomeric purity as well as structure determination.

Purification was done using standard column chromatography. This was the most challenging step as well as crucial step of the whole procedure. We used several different methods, from the simple to the more refined as we experimented with various conditions. The main complication we found was that the axial pyridine tends to be displaced by groups on the surface of the silica gel, which often resulted in the compound getting stuck on the column. Our first generation approach consisted in adding small amounts of pyridine to the eluent. This had the drawback of speeding up the elution of the compound so that very small fractions had to be taken and analyzed by UV-Vis. Fraction with the same Soret positions were then grouped together and further analyzed by ESI-MS. This approach yielded pure compounds, but was extremely time comsuming.

We then switched to a second generation approach in which silica gel was deactivated by adding water in certain proportions. (Actually, an excess of water was added and the silica gel was

Figure 5.1. Typical ESI-MS patterns for some partially brominated corroles. The left column shows the full spectrum, while the right column shows the detailed isotopic pattern.

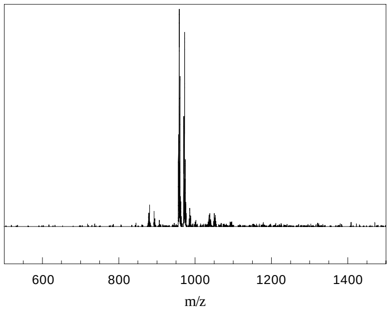

(Br-tpfc)Ga

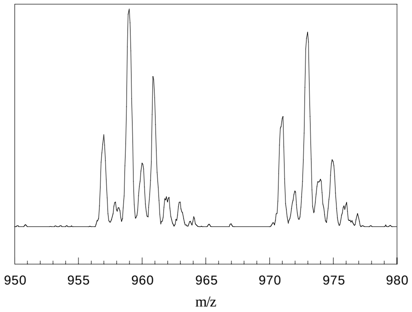

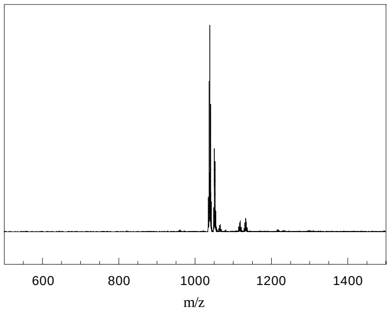

(Br$_2$-tpfc)Ga

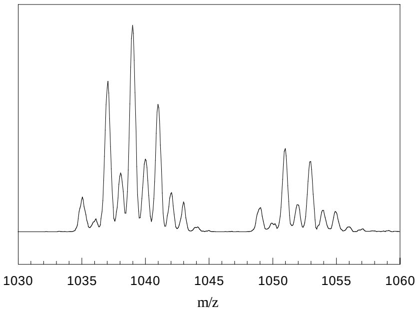

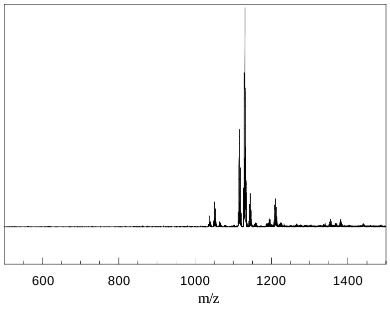

(Br$_3$-tpfc)Ga

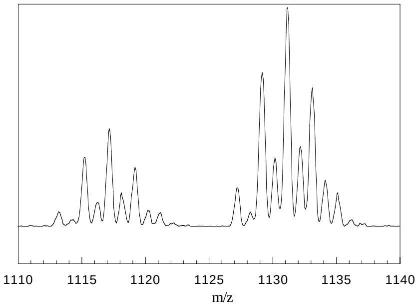

dried at 60 ˚C for 4 hours.) Using those conditions, we were able to elute separate bands, using increasingly polar solvents. Upon MS analysis, the pure bands were kept, and the mixed bands were subjected to further column chromatography using the same conditions. All in all, we were successful in isolating 4 different brominated compounds. Other compounds are probably formed, but their yields must be such as to make their isolation difficult using conventional chromatography.

Determination of the structure of partially brominated corroles

The low symmetry of the corrole macrocycle results in four different signals in the pyrrole region in its ^{1}H NMR spectrum. This is in contrast to porphyrins where all β protons are equivalent. We have adopted the following nomenclature for the corrole protons: the pyrroles linked by the direct carbon –carbon bond are termed A pyrroles, whereas the pyrroles linked by a meso carbon are termed B (see Figure 5.2a). Thus the protons are labeled A, A’ for pyrrole A, and B, B’ for the other pyrrole. Looking at the proton-proton J couplings, two different constants appear (J_1= 3.9 Hz, J_2= 4.4 Hz). We can therefore identify the signals which correspond to protons on the same pyrrole unit (Figure 5.2b). It is, however, not possible to assign any of the signals to either the A pyrrole or the B pyrrole based on the 1-D spectrum alone.

2-D NMR has been successfully used to assign the structure of other complex macrocycles for which no X-ray structures were available, F430 being a prime example. In that case, a combination of 1H-HMBC and 1H-HMQC was used. Briefly, 1H-HMQC (proton detected Heteronuclear Multiple Quantum Correlation spectroscopy) looks at correlations between 1H and 13C separated by a single bond. The main advantage of this technique over the more conventional magnetization transfer experiments is that magnetization is transferred from proton to carbon and back to proton, so that detection can be effected in the proton frequency, which increases the sensitivity. In the same vein, 1H-HMBC (proton detected Heteronuclear Multiple Bonds multiple quantum Correlation) looks at correlations over 2-3 bonds.

We first acquired a 13C spectrum of (tpfc)Ga(py) (Figure 5.3). The spectrum displays 8 peaks corresponding to α and β carbons, 3 peaks corresponding to the pyridine carbons, two signals corresponding to the meso positions, and weak signals due to the fluorophenyls.

Figure 5.2a. Labeling scheme for the corrole protons.

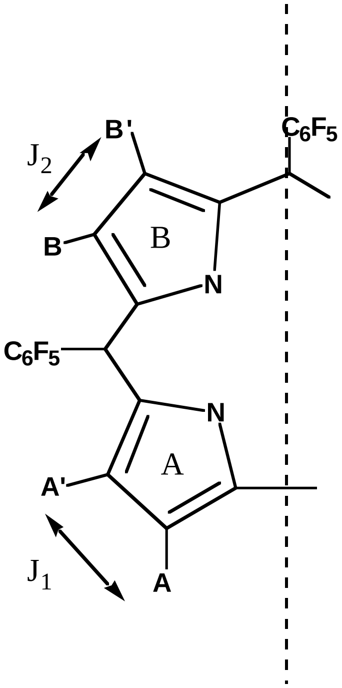
J2
B'
C6F5
B
B
N
C6F5
N
A
A'
J1
A

Figure 5.2b. ^{1}H NMR spectrum of (tpfc)Ga(py) in CH_2Cl_2 at room temperature.

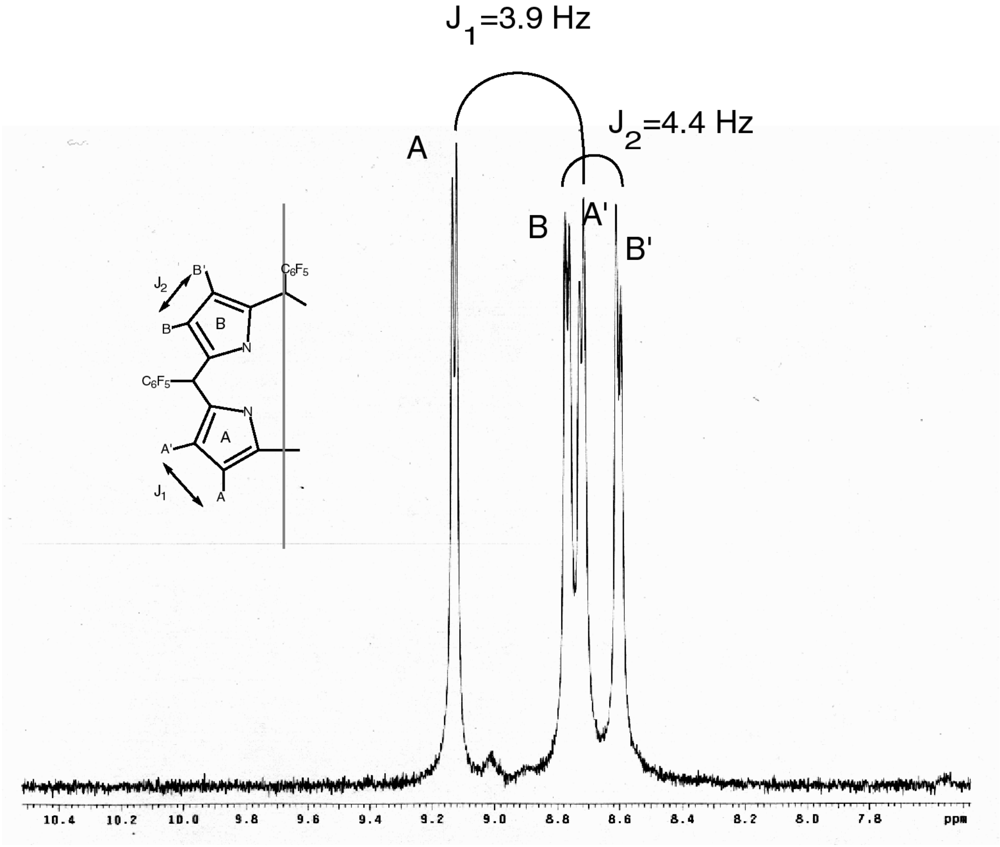
J1=3.9 Hz
J2=4.4 Hz
A
B
A'
B'
J2
B'
B
C6F5
N
C6F5
N
A
A'
A
J1
10.4
10.2
10.0
9.8
9.6
9.4
9.2
9.0
8.8
8.6
8.4
8.2
8.0
7.8
ppm

Figure 5.3. ^{13}C NMR spectrum of (tpfc)Ga(py) in CH_2Cl_2 at room temperature.

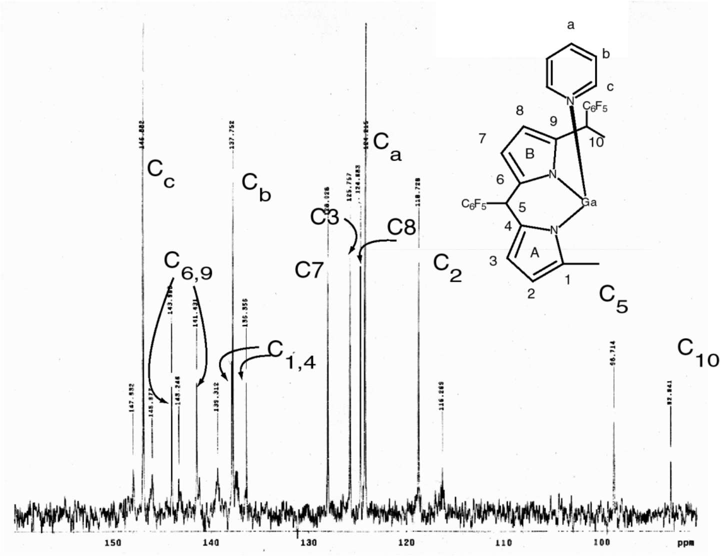
a
b
c
C_6F_5
8
9
7
10
B
6
N
C_6F_5
5
Ga
4
N
A
3
1
2
C_c
C_b
C_a
$C_{6,9}$
$C_{1,4}$
C3
C8
C7
C_2
C_5
C_{10}
147.932
146.882
145.877
143.246
141.431
139.312
137.752
136.356
128.026
125.757
124.683
118.728
116.289
98.714
92.841
150
140
130
120
110
100
ppm

Figure 5.4. HMQC spectrum of (tpfc)Ga(py) in CH_2Cl_2 at room temperature.

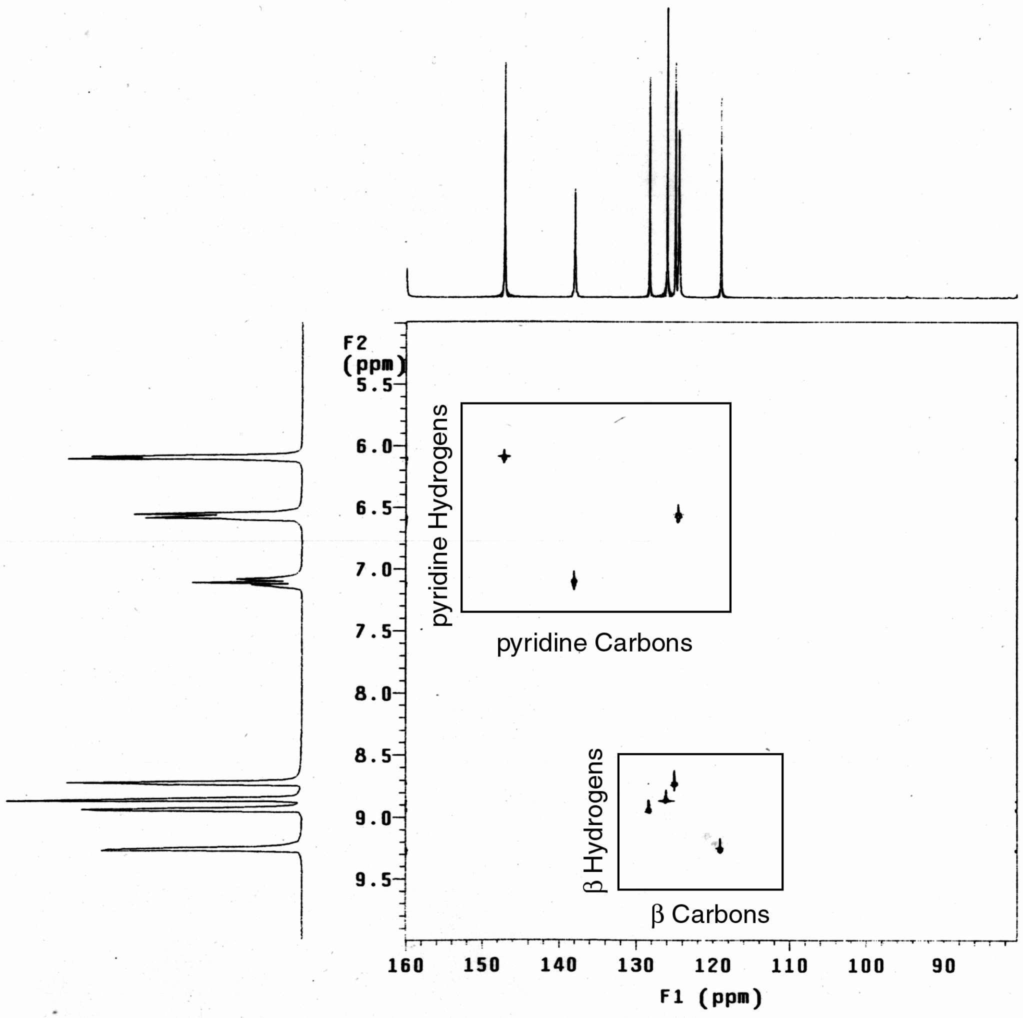
F2
(ppm)
5.5
6.0
6.5
7.0
7.5
8.0
8.5
9.0
9.5
pyridine Hydrogens
pyridine Carbons
β Hydrogens
β Carbons
160
150
140
130
120
110
100
90
F1 (ppm)

Figure 5.5. HMBC spectrum of (tpfc)Ga(py) in CH_2Cl_2 at room temperature.

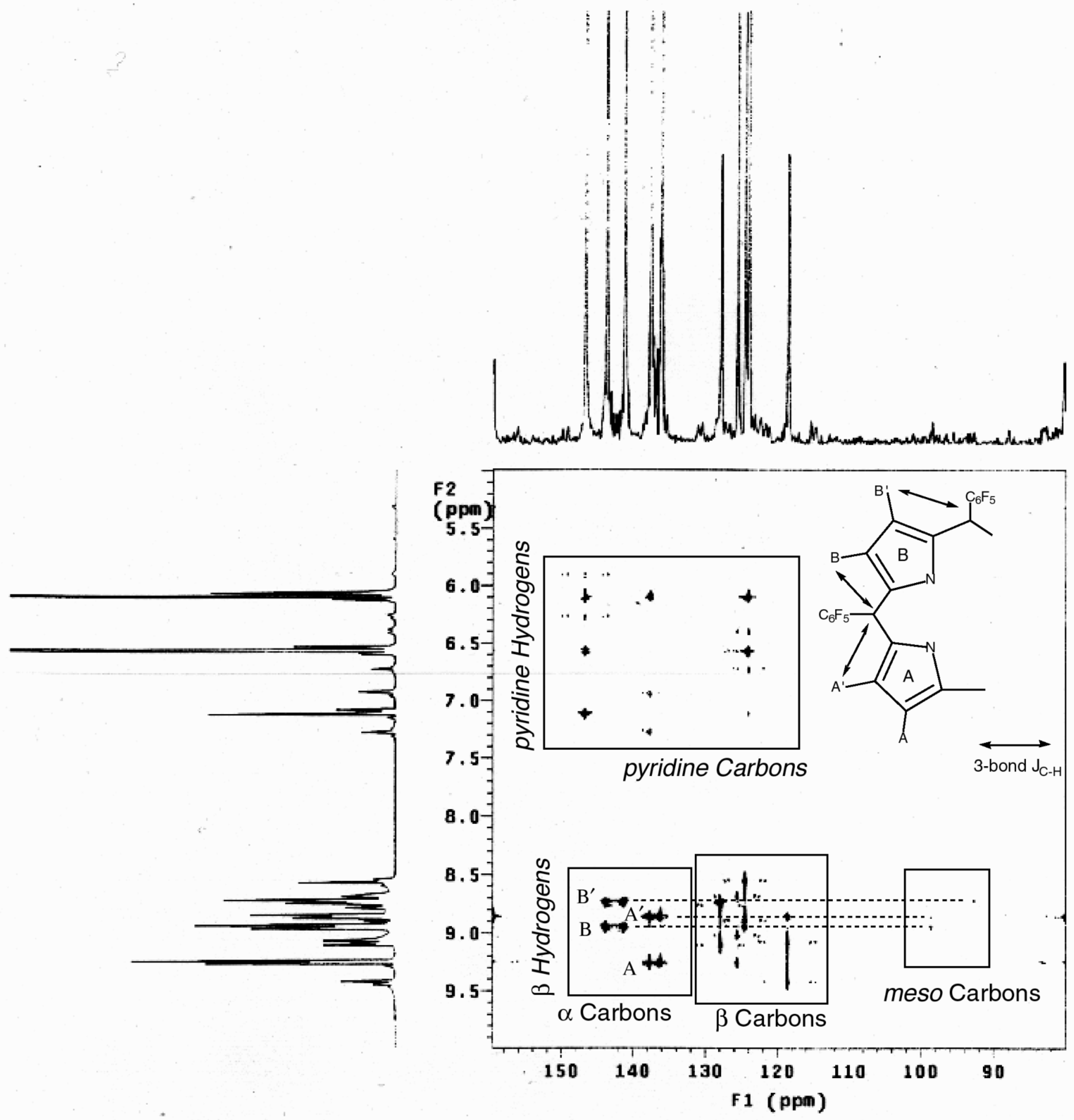
F2 (ppm)
5.5
6.0
6.5
7.0
7.5
8.0
8.5
9.0
9.5
pyridine Hydrogens
pyridine Carbons
β Hydrogens
B′
B
A′
A
α Carbons
β Carbons
meso Carbons
B′
C6F5
B
B
N
C6F5
A′
A
N
A
A
3-bond JC-H
150
140
130
120
110
100
90
F1 (ppm)

The HMQC spectrum merely shows correlations between the β carbons and their corresponding protons (Figure 5.4). It does not allow us to determine the structure. However HMBC gives us a lot more information (Figure 5.5). It contains three different regions, corresponding to α, β and meso carbons. HMBC would ideally suppress all one bond correlations. Often, those correlations are still visible, since they are so much more intense. Since the acquisition is done without decoupling (as opposed to HMQC), single bond correlations appear as streaks, while multiple bond correlations appear as single dots. This allows us to ignore the β region as being single bond correlations.

The α carbon region allows us to confirm the pairing of the pyrrole protons as deduced from the 1-D proton NMR. The critical information is contained in the weak meso region: one meso carbon is coupled to one proton while the other one is coupled to two. Since those are three bond correlations, the single meso can only couple to B', while the double meso signal couples to B and A'. This allows us to assign the B' proton uniquely, and we use the alpha region to assign B. From there we use the double meso signal to find A'. The remaining signal is assigned to A.

Having assigned the spectrum of the parent compound, we can now tackle the problem of determining the structure of the bromine-substituted compounds. All the 1-D spectra show clearly defined peaks, which suggest that there are no mixtures of isomers present. (Br-tpfc)Ga(py) has seven distinct signals: six doublets and one singlet. Using the chemical shifts, we can identify the B and B' protons. Note that both are split, which indicates a loss of mirror symmetry of the corrole ring. The splitting is more pronounced for the B protons, suggesting that they are closer to the site of bromination. This fact is also apparent in the larger upfield shift of the B protons compared to the B' (Figure 5.6).

The lone singlet is assigned to the proton next to the site of substitution. This is identified as the A proton due to its chemical shift. Note again the slight upshift from the non-substituted position. The remaining two doublets are associated with a single A and a single A’ proton, respectively. This identifies the site of bromination as A’.

In assigning the more substituted compounds, we take into consideration that all two brominated compounds have to go through the 1-Br stage first. Sequential bromine substitution is well known in aromatic chemistry as well as in porphyrin chemistry. (Br_2-tpfc)Ga(py) presents a symmetrical spectrum. The logical conclusion is that the compound has both A’ sites brominated (Figure 5.6). The next higher level of bromination, (Br_3-tpfc)Ga(py),

Figure 5.6. ^{1}H NMR spectra of : a) (Br-tpfc)Ga(py), b) (Br_2-tpfc)Ga(py), and c)(Br_3-tpfc)Ga(py) in CH_2Cl_2 at room temperature.

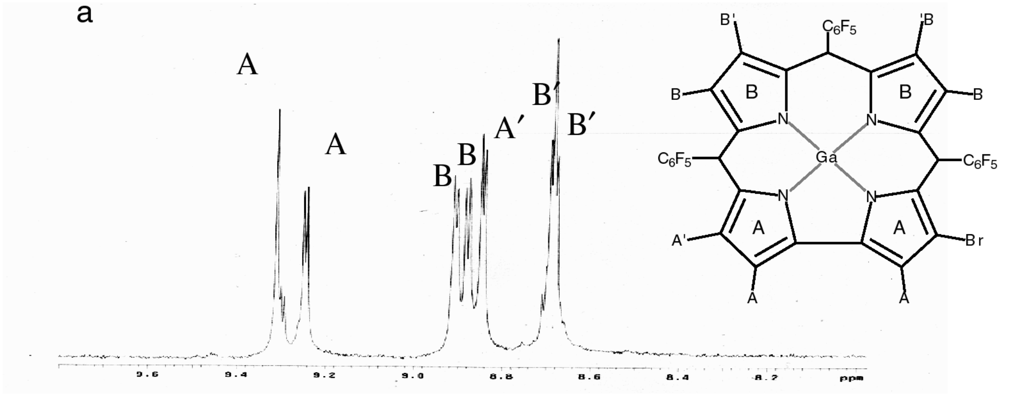
a
A
A
B
B
A′
B′
B′
9.6
9.4
9.2
9.0
8.8
8.6
8.4
8.2
ppm
B'
C6F5
B
B
B
B
B
C6F5
N
N
Ga
C6F5
N
N
A'
A
A
Br
A
A

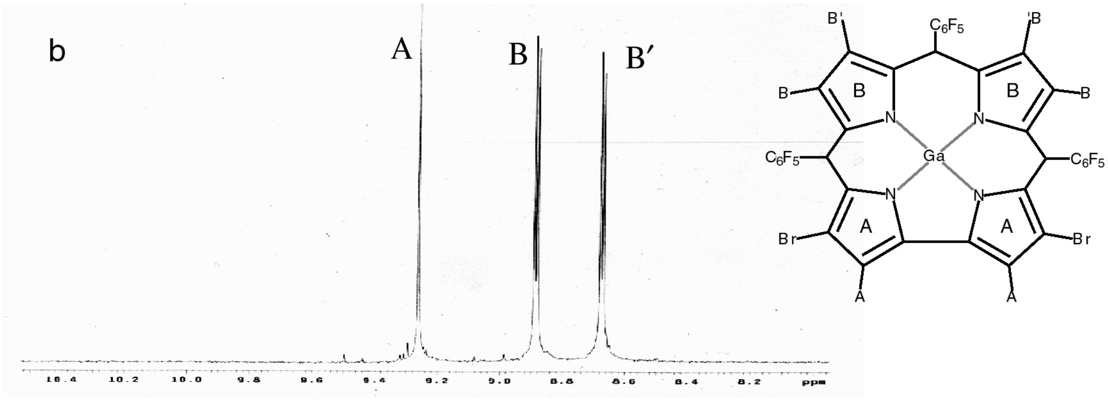
b
A
B
B′
10.4
10.2
10.0
9.8
9.6
9.4
9.2
9.0
8.8
8.6
8.4
8.2
ppm
B'
C6F5
B
B
B
B
B
C6F5
Ga
C6F5
Br
A
A
Br
A
A

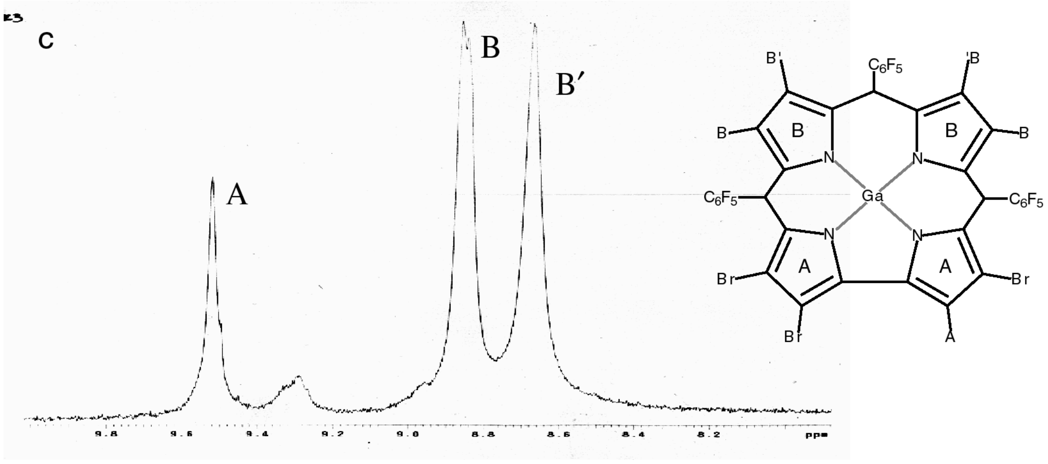
c
B
B′
A
9.8
9.6
9.4
9.2
9.0
8.8
8.6
8.4
8.2
ppm
B'
C6F5
B
B
B
B
B
C6F5
Ga
C6F5
Br
A
A
Br
Br
A

shows a broadening of the peaks, and a halving of the intensity of the most deshielded signal. We assign this to A, A’,A’ substitution. The break in symmetry is apparent in the broadening of all the peaks in the spectrum, suggesting a split. This split is not nearly as dramatic as for (Br-tpfc)Ga(py), mainly because the difference in electronegativity between both sides is small.

Finally, (Br_7-tpfc)Ga(py) only has a single peak in its spectrum, which precludes structural determination via the above methods. We have thus not assigned the site of the lone proton in this compound.

Electrochemistry of brominated corroles

Substituted porphyrins with various metals have been widely studied by electrochemical methods. This section is not intended to be a review of the field, but rather a summary of the most important conclusions. There is in general a shift in E^{ox}/E^{red} with increasing substitution. The relationship is non-linear, with a pronounced maximum for substitution numbers 4-6 aproximatively. [7] Ligand centered processes are affected to a much larger extent than metal centered processes. The best examples occur with nonelectroactive metals, like zinc. Non-linearity is caused by increased distortion due to steric repulsion between substituents. This is pronounced in the case of the heavier halogens. The importance of steric effects can be quantified by looking at the difference between the actual curve and a linear extrapolation using only the lower (1-3) substitution numbers. Steric effects become non-negligible past the maximum point (about 4-6 substituents, depending on the compound).

The trianionic nature of corroles makes gallium a better choice for a study of electronic effects. All reactions show two clean peaks corresponding to ligand oxidation and reduction, respectively (Figure 5.7).

The shift of E^{ox}/E^{red} with respect to substituent is perfectly linear, 49 and 51 mV/Br, respectively. This is comparable to the numbers obtained for $TPPFe^{III}$ for example (40 mV/Br). [9] The electronic effect seems to be about 25% stronger in corroles. There is, however, a total absence of steric effects, as shown by the linearity of the shift up to substitution number 7. This suggests to us that there is no deformation of the macrocycle, as there is in porphyrins, where saddling and ruffling are routinely observed.

Figure 5.7. a) Typical cyclic voltamogram of (tpfc)Ga(py) in 0.1M $TBAPF_6/CH_2Cl_2$; b) dependence of E^{ox} and E^{red} on the number of bromine substituents.

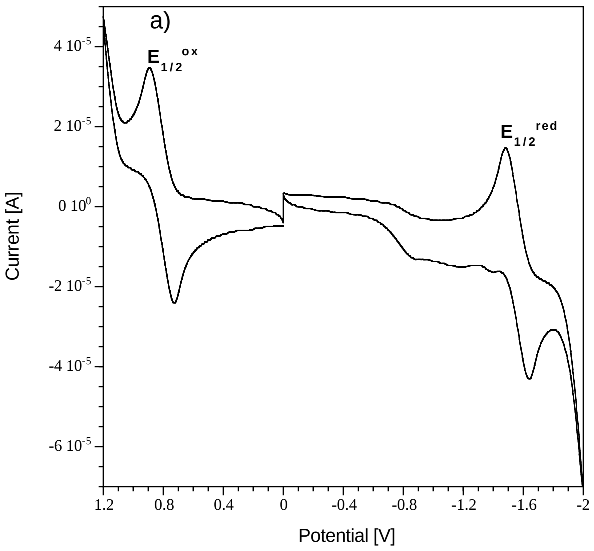
a)
E1/2 ox
E1/2 red
Current [A]
4 10-5
2 10-5
0 100
-2 10-5
-4 10-5
-6 10-5
1.2
0.8
0.4
0
-0.4
-0.8
-1.2
-1.6
-2
Potential [V]

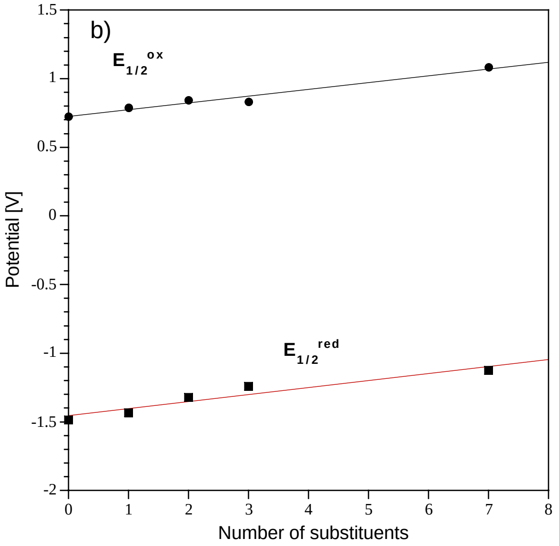
b)
E1/2 ox
E1/2 red
Potential [V]
1.5
1
0.5
0
-0.5
-1
-1.5
-2
0
1
2
3
4
5
6
7
8
Number of substituents

Steric deformation in corroles

The above measurements suggest that corroles resist out-of-plane deformations of the macrocycle. Over the past year, the number of corrole compounds whose x-ray structure has been determined has increased considerably. A common point among these structures is the near planarity of the ligand framework itself. There is very little deformation, contrary to what is observed in porphyrins. Although the range of compounds examined in the case of corroles is not as extensive, there is a definite trend in that direction.

The recent report of the structure of (Br_8-tppc)Co(PPh_3) supports this hypothesis.[13] When compared with a compound with less bulky substituents , (octamethylcorrolato) Co, the macrocyclic deformation is nearly the same.This is not the case if one compares the two corresponding porphyrin compounds, where the bromo substituents induce more deformation than methyls.

The cause for such robustness to deformation in corroles is not known, but we propose the following: since the main deformation causing interaction is between meso phenyl groups and adjacent substituents on β positions, anything that reduces that interaction would lessen the tendency toward planar deformation. The direct pyrrole-pyrrole link in corroles leads to a greater separation between the β and meso positions, as measured by the β-center-β angle. We propose that this is the main reason for the lack of steric deformation in corroles.

As a consequence, the maximum electronic effect is observed for the maximum substitution number in the case of corroles.

UV-Vis of partially brominated corroles

The UV-visible spectra of brominated corroles are similar to that of the parent compound. They exhibit a characteristic Soret band as well as two Q bands. The bands also red-shift, about 2 nm for the Soret. The Q bands show more complex behavior. The red Q band (Qb) does not markedly shift, whereas the blue one (Qa) displays a 4 nm shift per bromine, which is about double that of the Soret band (Figure 5.8). Also, the relative intensities of Qa versus Qb change, with Qa becoming more intense relative to Qb with increasing substitution.

The spectra of porphyrins are generally interpreted in terms of the Gouterman four-orbital model, where the HOMOs are nearly degenerate a_{2u} and a_{1u} orbitals, while the LUMO consists of the e_g pair. The direct electronic transitions from a_{1u} (a_{2u}) to e_g mix via

Figure 5.8. UV-Vis spectrum of brominated gallium corroles in CH_2Cl_2. Soret and Q bands are shown in inserts.

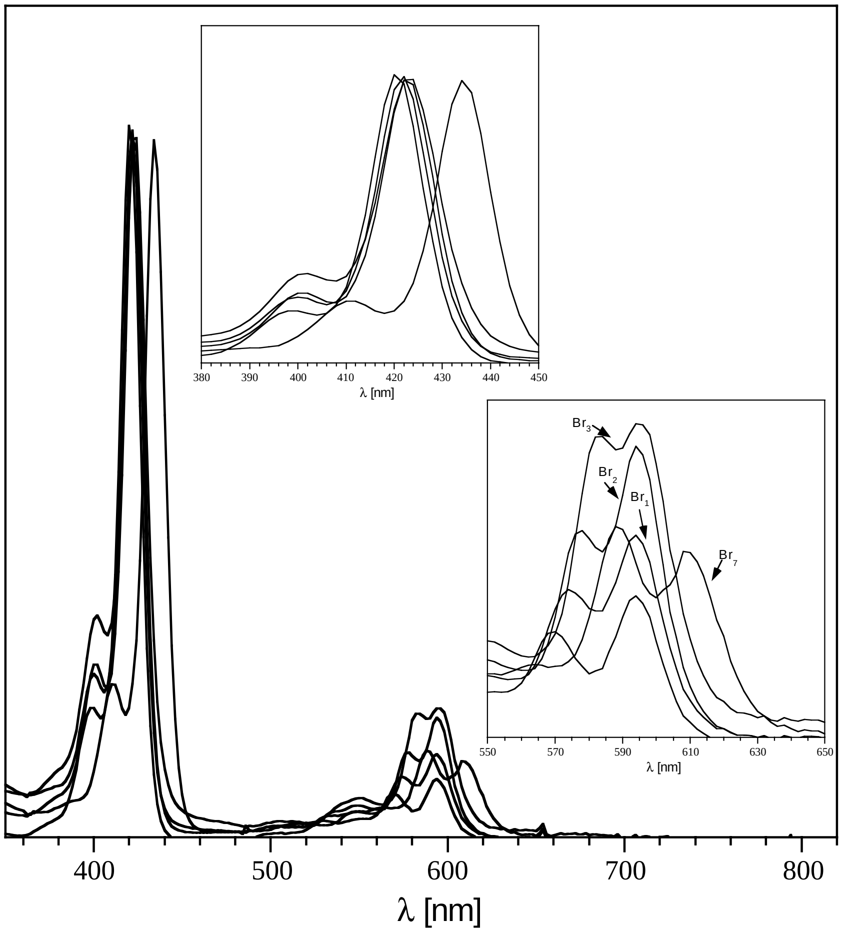
380
390
400
410
420
430
440
450
λ [nm]
Br3
Br2
Br1
Br7
550
570
590
610
630
650
λ [nm]
400
500
600
700
800
λ [nm]

configuration interaction to give the observed B and Q bands. The Q band itself has structure, the lowest band being the fundamental Qa (Q(0,0)), while the blue Q band Qb (Q(1,0)) corresponds to an envelope of vibronically allowed peaks. Furthermore, the intensity borrowed by Q(1,0) from the B (or Soret) band is nearly constant for porphyrins, [14]leading to a relationship between ε(Q(0,0))/ε(Q(1,0)) and the separation between a_{1u} and a_{2u} that leads to this ratio becoming larger as the separation between those orbitals decreases. [15]

Electrochemical measurements give direct access to the e_g pairs as well as the highest of either a_{1u} or a_{2u}. By combining those results, with the positions of the B and Q bands, the relative separation between a_{1u} and a_{2u} can be estimated. [15] Applying this method to a series of brominated zinc porphyrins shows that the gap increases with increasing substitution, the effect being more pronounced in the lowest orbital. There is also a very definite curvature in the shift. This is again attributed to steric effects. From this plot, it is clear that the orbitals are affected unequally by β substitution. This is consistent with a sketch of the molecular orbitals that shows a_{1u} as having more density on the β positions.

There is no reason for this model not to apply to corroles. The lowering in symmetry does split the e_g orbital and changes the labels of the two lowest HOMOs to b_1 and a_2, but the general framework remains the same. By applying the above method to the spectral and electrochemical data, we find that the gap between b_1 and a_2 increases with increasing bromination. This is in line with the relative intensities of the Q bands, which again indicate increased separation of the lowest HOMOs. We plot the relative change in gap energy in Figure 5.9. Note that both orbital energies shift linearly with increasing bromination, with the higher orbital slightly more affected.

Our findings stand in stark contrast to the situation for zinc porphyrins, where there is a large difference in the effects on the two HOMOs, due mainly to steric deformations of the macrocycle.

Conclusion

We have shown that partially brominated corroles can be readily prepared and characterized. Measurements of their electrochemical and spectroscopic properties emphasize the differences between porphyrins and corroles in regards to β substitution. The latter does not lead to distortion of the macrocycle. Estimates of the energies of frontier orbitals shows that, like zinc porphyrins, the gap between the two HOMOs increases upon bromination in a linear fashion, with both orbitals being affected to the same extent.

Figure 5.9. Relative shift of the two HOMOs in (TPP)Zn (a) and (tpfc)Ga(py) (b).

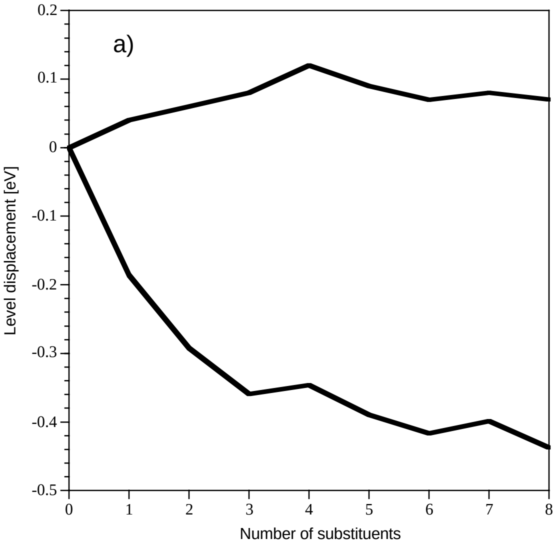
a)
Level displacement [eV]
0.2
0.1
0
-0.1
-0.2
-0.3
-0.4
-0.5
0
1
2
3
4
5
6
7
8
Number of substituents

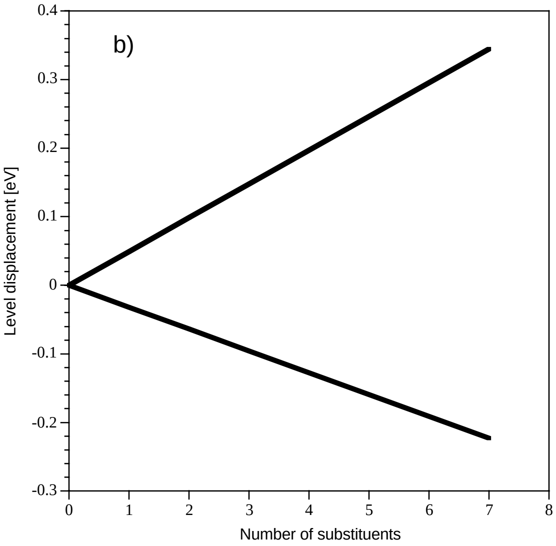
b)
Level displacement [eV]
0.4
0.3
0.2
0.1
0
-0.1
-0.2
-0.3
0
1
2
3
4
5
6
7
8
Number of substituents

References

(1) Grinstaff, M. W.; Hill, M. G.; Labinger, J. A.; Gray, H. B. *Science* **1994**, *264*, 1311.

(2) Birnbaum, E. R.; Grinstaff, M. W.; Labinger, J. A.; Bercaw, J. E.; Gray, H. B. *J. Mol. Catal. A* **1995**, *104*, L119.

(3) Bottcher, A.; Grinstaff, M. W.; Labinger, J. A.; Gray, H. B. *J. Mol. Catal. A* **1996**, *113*, 191.

(4) Chang, C. J.; Labinger, J. A.; Gray, H. B. *Inorg. Chem.* **1997**, *36*, 5927.

(5) D'Souza, F.; Zandler, M. F.; Tagliatesta, P.; Ou, Z.; Shao, J.; Van Caemelbecke, E.; Kadish, K. M. *Inorg. Chem.* **1998**, *37*, 4567.

(6) D'Souza, F.; Villard, A.; Van Caemelbecke, E.; Frazen, M. M.; Boschi, T.; Tagliatesta, P.; Kadish, K. M. *Inorg. Chem.* **1993**, *32*, 4142.

(7) Kadish, K. M.; D'Souza, F.; Villard, A.; Autret, M.; Van Caemelbecke, E.; Bianco, P.; Antonini, A.; Tagliatesta, P. *Inorg. Chem.* **1994**, *33*, 5169.

(8) Kadish, K. M.; Li, J.; Van Caemelbecke, E.; Ou, Z.; Guo, N.; Autret, M.; D'Souza, F.; Tagliatesta, P. *Inorg. Chem.* **1997**, *36*, 6292.

(9) Tagliatesta, P.; Li, J.; Autret, M.; Van Caemelbecke, E.; Villard, A.; D'Souza, F.; Kadish, K. M. *Inorg. Chem.* **1996**, *35*, 5570.

(10) Callot, H. J. *Bull. Soc. Chim. Fr. II* **1974**, *7-8*, 1492.

(11) Ghosh, A.; Jynge, K. *Chem. Eur. J.* **1997**, *3*, 823.

(12) Bendix, J.; Dmochowski, I. J.; Gray, H. B.; Mahammed, A.; Simkhovich, L.; Gross, Z. *Angew. Chem. , Int. Ed.* **2000**, *39*, 4048.

(13) Paolesse, R.; Nardis, S.; Sagone, F.; Khoury, R. G. *J. Org. Chem.* **2001**, *66*, 550.

(14) Perrin , H. M.; Gouterman, M.; Perrin, C. L. *J. Chem. Phys.* **1969**, *50*, 4137.

(15) Binstead, R. A.; Crossley, M. J.; Hush, N. S. *Inorg. Chem.* **1991**, *30*, 1259.